

Original Research Article

Geothermal Gradient, Curie Point Depth and Heat Flow Determination of Some Parts of Lower Benue Trough and Anambra Basin, Nigeria, Using High Resolution Aeromagnetic Data

Abstract

Background and Objective: This study, which is bounded within Latitude $6^{\circ} 00' - 6^{\circ} 30' N$ and Longitude $7^{\circ} 00' - 7^{\circ} 30' E$ with an approximate area of about 3025 km^2 within parts of lower Benue trough and Anambra basin of Nigeria, aims at outlining the regional temperature distribution and delineating areas that are geo thermally responsive by determining: the heat change per unit distance, the heat flowing from the earth's interior to the outer surface and the deepest depth at which the minerals loss their magnetic properties within the study area without any heat data. **Materials and Methods:** For the aim to be achieved, the data was subjected to quantitative analysis with the aid of the WingLink, ArcGIS, Origin Pro 8, Ms Excel and sulfer 10 software's. Regional-residual was applied on the total magnetic intensity map and thereafter the residual divided into sixteen (16) overlapping windows. Spectral depth analysis was performed upon the overlapping windows and this revealed depth due to low frequency and high frequency components. The depths due to the low frequency components exemplify the Curie depth point (CPD). **Results:** The average sedimentary thickness or the average depth due to the low frequency part was ascertained to be -5 km while the geothermal and heat flow varies from $-25.2 \text{ }^{\circ}\text{Ckm}^{-2}$ to $-38.9 \text{ }^{\circ}\text{Ckm}^{-2}$ and from -64.4 mWm^{-2} to -97.3 mWm^{-2} but with average values of $-32.1 \text{ }^{\circ}\text{Ckm}^{-2}$ and -80.1 mWm^{-2} respectively. **Conclusion:** These results suggest alternative geothermal energy resource to be plausible within windows 2, 4, 8, 10, 12, 15 and 16 and presence of some amount of sedimentary thickness within the area of study.

Keywords: *WingLink, ArcGIS, CPD, Windows, Heat flow, Geothermal gradient, HRAM, Raster, CSV.*

31 INTRODUCTION

32 Aeromagnetic technique is a type of geophysical technique in which a magnetometer is
 33 towed behind an aircraft. Aeromagnetic data has been, and will continue to be, handy in the
 34 geophysical and geological investigation of the earth's interior. Umeanoh (2015) asserted that
 35 aeromagnetic data can be used in mapping magnetic basement in sedimentary rocks and
 36 delineating igneous bodies within sedimentary sections as well as locating lineaments and
 37 structures which could be possible host to varying earth resources like groundwater, minerals
 38 and hydrocarbon. Aeromagnetic method has been used majorly for the estimation of depth to
 39 basement and thickness of sediments within sedimentary basins. Although this method was
 40 used in mapping igneous and metamorphic rocks and structures related to them because these
 41 rocks have high magnetization compared to other rocks^{2,3}.

42 Despite being used in delineating architectural framework of the earth's subsurface geology,
 43 the aeromagnetic method, can be applied successfully in defining geothermal gradient of an
 44 area via spectral analysis. It was pointed out that the assessment of variations of the Curie
 45 isotherm of an area can provide valuable information about the regional temperature
 46 distribution at depth and the concentration of subsurface geothermal energy⁴. The Curie-
 47 point temperature varies from region to region, depending on the geology of the region and
 48 mineralogical content of the rocks. Therefore, one normally expects shallow Curie-point
 49 depths in regions that have geothermal potential, young volcanism and thinned crust^{4,5}. In
 50 order to determine the Curie-point depths, i.e. the bottom of the magnetized rocks, and to
 51 map these depths, a frequently used method is the analysis of magnetic data.

52
 53 The Benue trough is based on lead-zinc mineralization, limestone deposits, coal deposits,
 54 coal deposits, pyroclastics, brine spring and brine Lake¹. Interestingly, the Benue trough
 55 especially the lower Benue trough has been studied deeply by researchers, students and
 56 private organizations using either a combination of magnetic, gravity or any other
 57 geophysical technique for mineral exploration. Currently aeromagnetic studies has received
 58 the kind of attention other geophysical techniques have received. Many authors⁶⁻⁹ have
 59 carried out studies on magnetic anomalies to estimate bottom depths of the related bodies for
 60 various purposes through the application of various techniques. However, some authors^{4,5}
 61 have also undertaken determination of Curie-point depths (CPD) within some major basins of
 62 the world.

63 In the present study, the objective is to estimate the average sedimentary thickness,
 64 geothermal gradient, Curie Point Depth (CPD) as well as the heat flow within the study area.
 65 This aids in viewing the thermal structure of the crust. The CPD nevertheless can be defined
 66 as the deepest level in the earth crust containing materials which creates discernible
 67 signatures in a magnetic anomaly map ¹¹. In other words, the further the depth, the material
 68 changes from a ferromagnetic material to a paramagnetic one. However, one of the important
 69 parameters that determine the relative depth of the Curie isotherm with respect to sea level is
 70 the local thermal gradient, that is, heat flow ¹². This Curie Isotherm, generally, has a
 71 temperature of $550^{\circ}\text{C} \pm 30^{\circ}\text{C}$ ¹¹. This point is assumed to be the depth for the geothermal
 72 source (magmatic chamber) where most geothermal reservoirs tapped their heat from in a
 73 geothermal environment. Measurements have shown that a region with significant
 74 geothermal energy is characterised by an anomalous high temperature gradient and heat flow
 75 ⁴. It is therefore expected that geothermally active areas would be associated with shallow
 76 Curie point depth ¹³. It is also a known fact that the temperature inside the earth directly
 77 controls most of the geodynamic processes that are visible on the surface ¹⁴. In this regard,
 78 Heat flow measurements in several parts of African continent have revealed that the
 79 mechanical structure of the African lithosphere is variable ¹⁵.

80 The very concept underlying magnetic prospecting is the existence of a magnetic dipole or
 81 monopoles within the rocks constituting the earth¹.

82 Magnetic force expression, F between two magnetic monopoles of strength P_1 and P_2 is given
 83 by:

84

$$85 \quad F = \frac{p_1 p_2}{\mu r^2} \quad 1$$

86 Where

87 P_1 and P_2 are dipoles

88 r is in meters and it is the distance between P_1 and P_2

89 μ is the free space permeability

90

91 The above Coulomb's equation is the basic underlying principle of magnetic prospecting.

92 Magnetic monopole, P_1 or P_2 exert force per unit pole strength and it can be expressed as:

$$93 \quad H = \frac{P}{r^2} \quad 2$$

94

95 Where

96

97 P is the magnetic monopole

98 r is the distance between the force in question and the magnetic monopole

99 H = strength of the magnetic field

100

101 Generally, the existence of a monopole has never been accounted for. Basically, magnetic
102 monopoles or dipole are made up of positive and negative poles separated by a distance. The
103 force produced and thus existing between monopoles can be estimated by vectorially adding
104 the forces generated by each of the monopoles or dipole. The force generated by a simple bar
105 magnetic can be compared to the force generated by a dipole.

106 .

107 Magnetic materials positioned within a magnetic field will acquire magnetic force and will
108 experience magnetic induction. Due to the inducing field, one can measure the strength of the
109 magnetic field known as the intensity of magnetization, J_i , induced on the material and this is
110 expressed as:

111

$$112 \quad J_i = kT \quad 3$$

113 Where

114 J_i is the magnetization

115 k = susceptibility of the magnetic material

116 T = inducing field.

117

118 LOCATION AND GEOLOGIC SETTINGS OF THE STUDY AREA

119 The study area is located in Enugu state and parts of Anambra state, south-east Nigeria. The
120 coordinates are Latitude $6^{\circ} 00' - 6^{\circ} 30' N$ and Longitude $7^{\circ} 00' - 7^{\circ} 30' E$. The study area falls
121 within the Lower Benue Trough and parts of Anambra basin. The Benue Trough generally
122 has been subdivided into three: the Upper Benue Trough at the NE Nigeria, the Middle
123 Benue Trough and the Lower Benue Trough. The Lower Benue Trough has somewhat
124 developed different tectonic history resulting in the formation of the Anambra Basin to the
125 west and Abakaliki Anticlinorium to the east¹.

The Anambra Basin remained a stable platform supplying sediments to the Abakaliki depression during a period of spasmodic phase of platform subsidence in the Turonian. Following the flexural inversion of the Abakaliki area during the Santonian uplift and folding, then the Anambra Basin was initiated. Four Cretaceous depositional cycles were recognized in the Lower Benue and each of these was associated with the transgression and regression of the sea¹⁷. The opening of the Atlantic Ocean in the Middle Albian to Upper Albian gave rise to the transgression of the first sedimentary cycle. The Asu River group which consist predominantly sandstone and shale was deposited at this time. Between the Upper Cenomanian and Middle Turonian, the second sedimentary deposition of the Ezeaku Shale occurred. The third sedimentary circle occurred from Upper Turonian to the Lower Santonian leading to deposition of the Awgu Shale and Agbani Sandstone. The fourth and final depositional phase took place during the Campanian-Maastrichtian transgression. It was at this time that the Nkporo Shale, Owelli Sandstones, Afikpo Sandstone, Enugu Shale as well as the coal measures including the Mamu Formation, Ajali Sandstone and Nsukka Formation was deposited¹⁷. Fig.1 shows the study area and the regional geology of the Lower Benue trough. The geological map (Fig 2) of the study was extracted from the regional geologic map and redigitized using the Arc GIS software for enhanced interpretation of the aeromagnetic map. Visually inspecting the map shows five main formations within the study area. These include: Nkporo Shale Formation, Mamu Formation, Ajali Formation, Nsukka Formation and Ameki Formation. The ages of the formations range from Maastrichtian to Campanian and to Eocene (Ameki formation).

MATERIALS AND METHODS

This research work made use of a digitized High Resolution Aeromagnetic (HRAM) data compiled by Fugro Airborn Service on behalf of the Nigerian Geological Survey Agency (NGSA) in 2009. The Composite Total Magnetic Intensity (CTMI) map with sheet number 301 was obtained in comma separated variable (CSV) format and in half degree sheet. The aeromagnetic data in CSV format was later transformed into a raster format (Fig 3). The high resolution survey was carried out at flight line spacing of 500 meters and at a ground clearance of about 100 meters while the tie line spacing was 2 km at flight line direction of NE-SW.

158 The acquisition of the HRAM data initially took place in Ogun state in the year 2003.
159 Thereafter, between year 2004 and 2009 the rest of the country was divided into project areas
160 referred to as Phases I and II covering 44% and 56% respectively of the total area. The raw
161 data was pre-processed using Oasis montaj software by the NGSA and was transmitted as
162 IGRF corrected total magnetic intensity (TMI) data and was also saved in CSV file format.

163

164

165

166

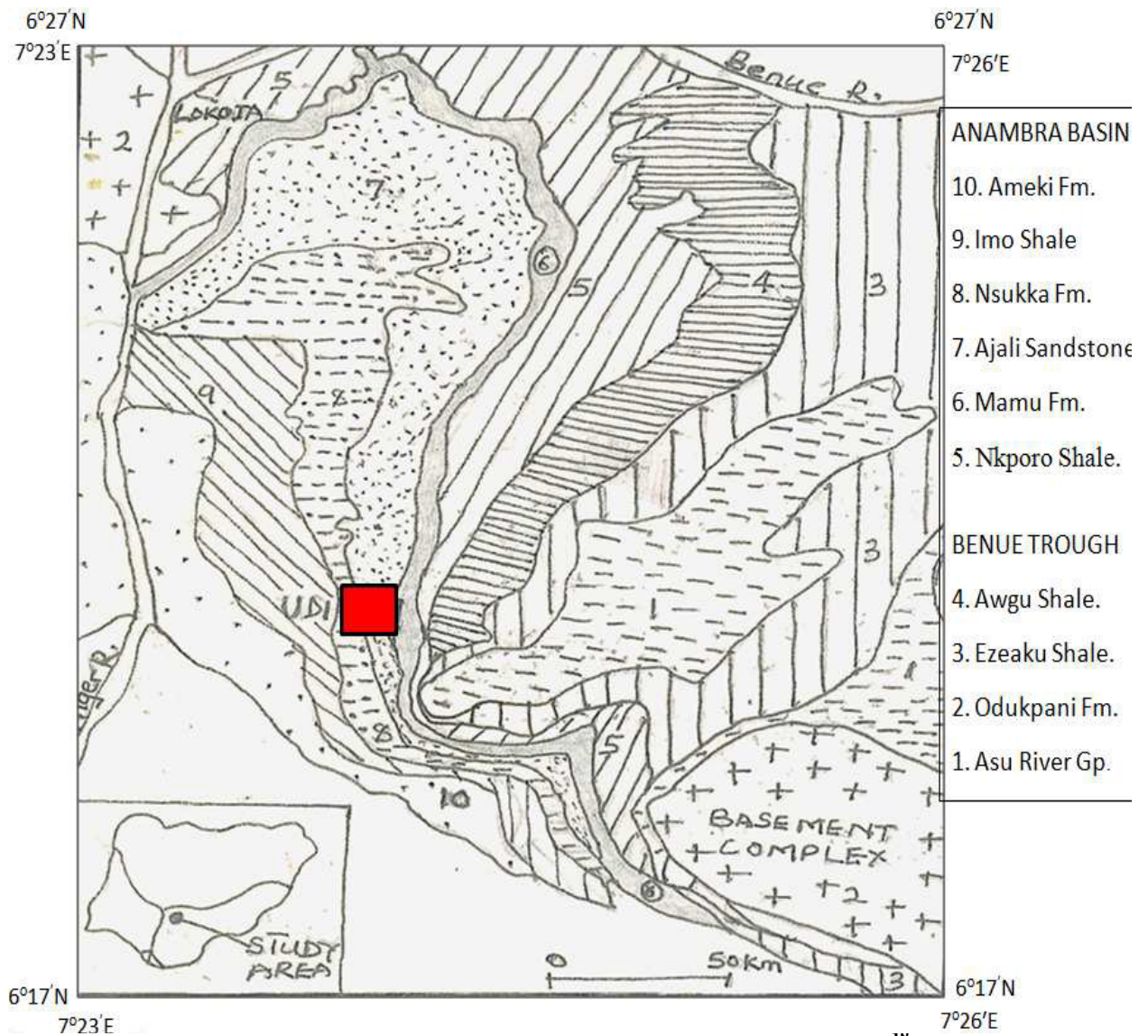


Fig.1: Regional Geology of the Lower Benue Trough showing the study area¹⁸

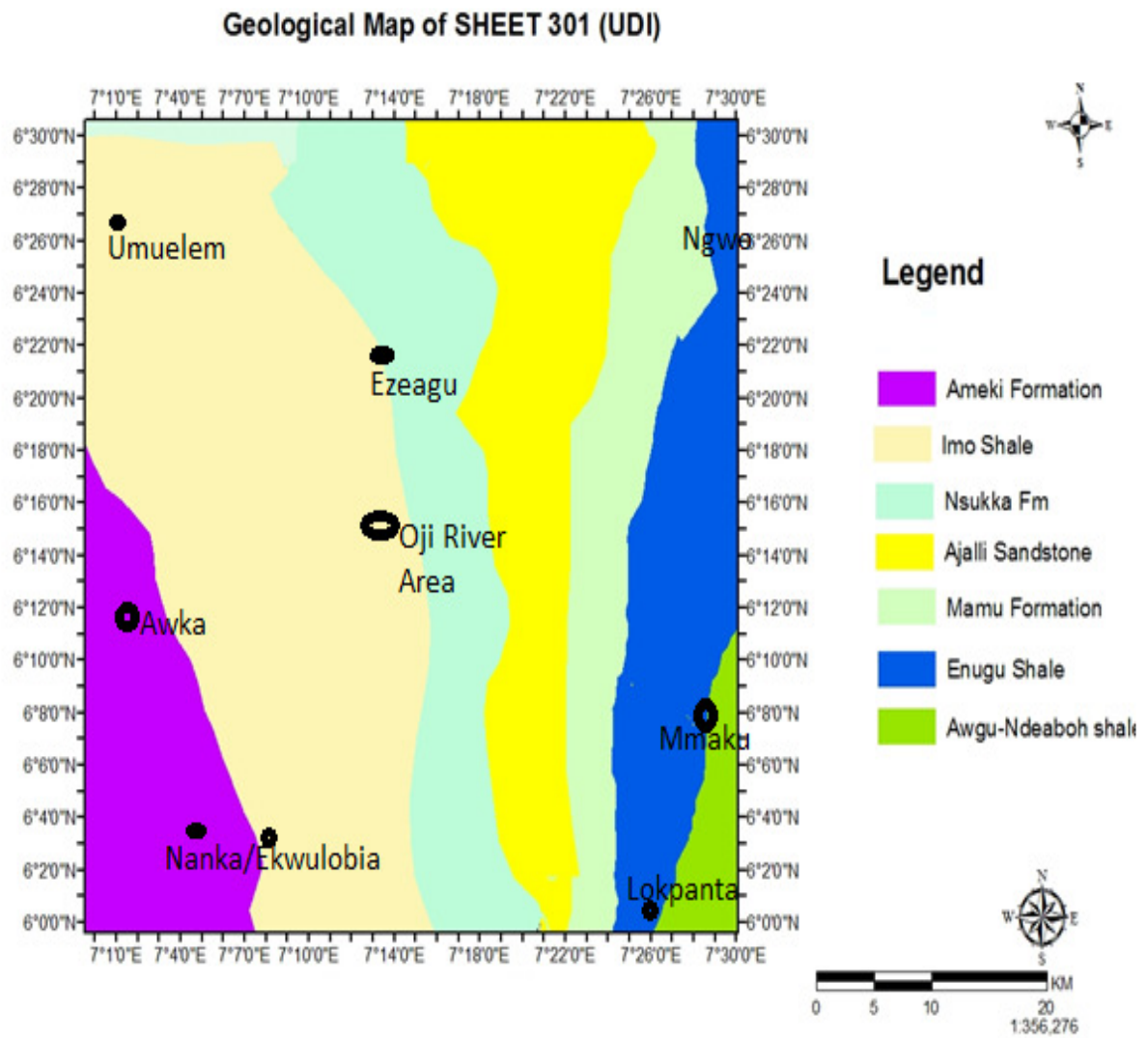


Fig. 2: Geologic Map of the Study Area (Sheet 301 and Re-digitized using the Arc GIS)

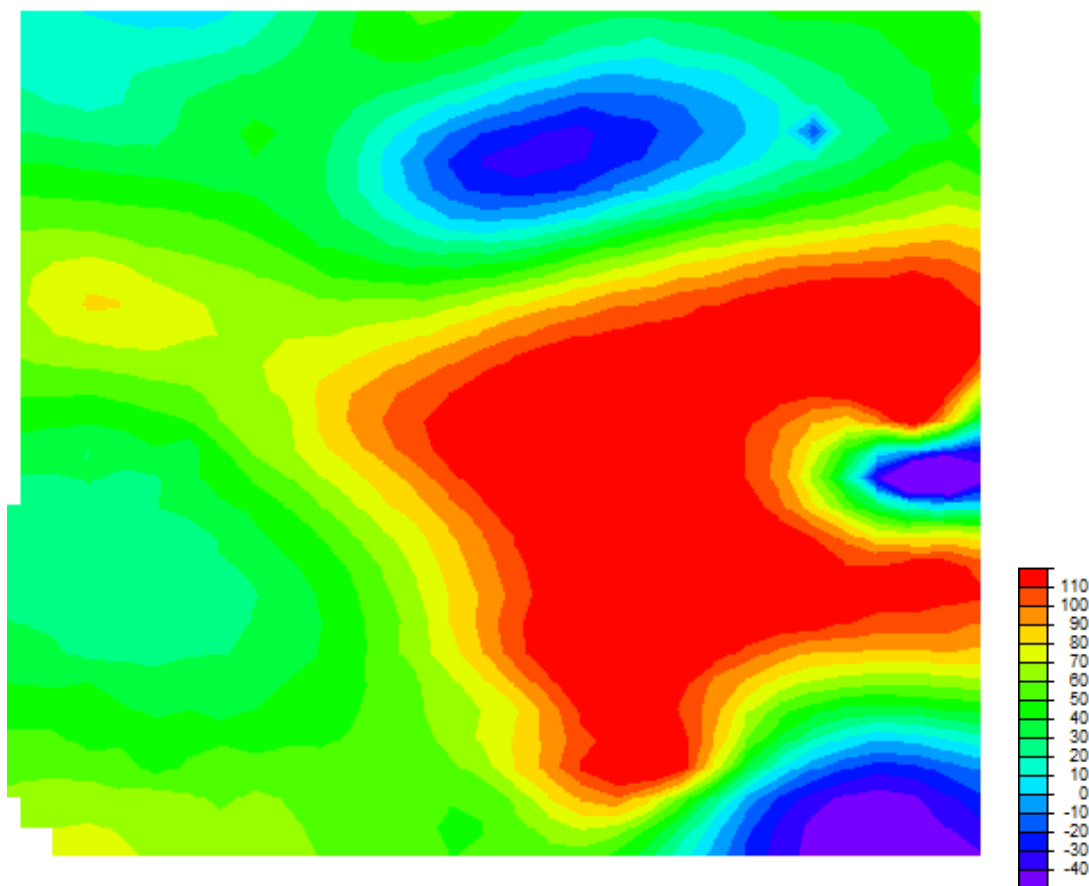


Fig 3: AEROMAGNETIC RASTER MAP OF THE STUDY AREA (nT)

For effective data analysis, processing and interpretation, the WingLink, ArcGIS softwares were used for qualitative interpretation while the MS excel, Surfer 10 and Origin Pro 8 Geophysical software's were used for quantitative interpretation. The data which was obtained in CSV format was opened and digitized in ESRI ArcGIS software for onward processing and interpretation. The data was processed and converted in a format usable by the WingLink visualization software with the aid of the ArcGIS. The digitization was done in grid of 1 km x 1 km spacing and values of TMI, X (latitude) and Y (longitude) were picked at the intersection of the grid nodes.

Manual digitization is the most elementary and least efficient method of digitisation, its accuracy when carefully done, compares favourably with other sophisticated methods using

computer programs¹⁴. The 1 km x 1 km grid points generated over 6000 sample points. The x and y show the coordinates while the z represents the TMI value at the point. This was implemented in ArcGIS 9.3 software and the xyz data was saved as MS Excel file format. The data saved as excel file format was thereafter imported into the Micro soft (MS) excel environment for band pass filtering. The band filtering was carried out so as to create sixteen (16) overlapping spectral windows upon which Fast Fourier Transform (FFT) was performed.

DEPTH DETERMINATION

The depth to sedimentary thickness and its morphology can be determined using spectral depth analysis. Spectral depth technique has being used by several authors in determining the thickness of sediments within their restricted area of study. Aside from the spectral depth method, other automated or semi automated techniques, like Euler Deconvolution, Improved Source Parameter imaging (ISPI), Werner Deconvolution and tilt angle, can as well be used in estimating depth to basement (that is, the thickness of sediments). Therefore, for this study, Spectral analysis is the basis for depth determination using the potential field aeromagnetic data of the study area. It was opined ¹⁹ that Spectral analysis has proved to be a powerful and convenient tool in the processing and interpretation of potential field geophysical data. It seeks to describe the frequency content of a signal based on a finite set of data. This technique is believed to provide rapid depth estimates from regularly spaced digital field data, no geomagnetic or diurnal corrections are necessary as these remove only low wave number components and do not affect the depth estimates which are controlled by the high wave number components of the observed field. This technique is based on the shape of the power spectrum for buried bodies with a susceptibility contrast. It is shown for simple bodies ²⁰ and for complex shaped bodies ⁷ that the depth to the center of mass of the body is easily obtained from the power spectrum of the magnetic field. If the spectrum is plotted on semi-log paper, the slope of the spectrum is equal to the depth to the center of mass. Extremely complex shapes and layering can, however, complicate the spectrum. The spectrum gives information primarily about the location of the top and bottom of a magnetic layer ²¹. Nevertheless, this research follows the assumption that magnetic basement is composed of a randomly distributed number of structures. Then by calculating the average of the spectra, the depth for all anomalous sources is determined and this is equivalent to that for a single body at the same depth.

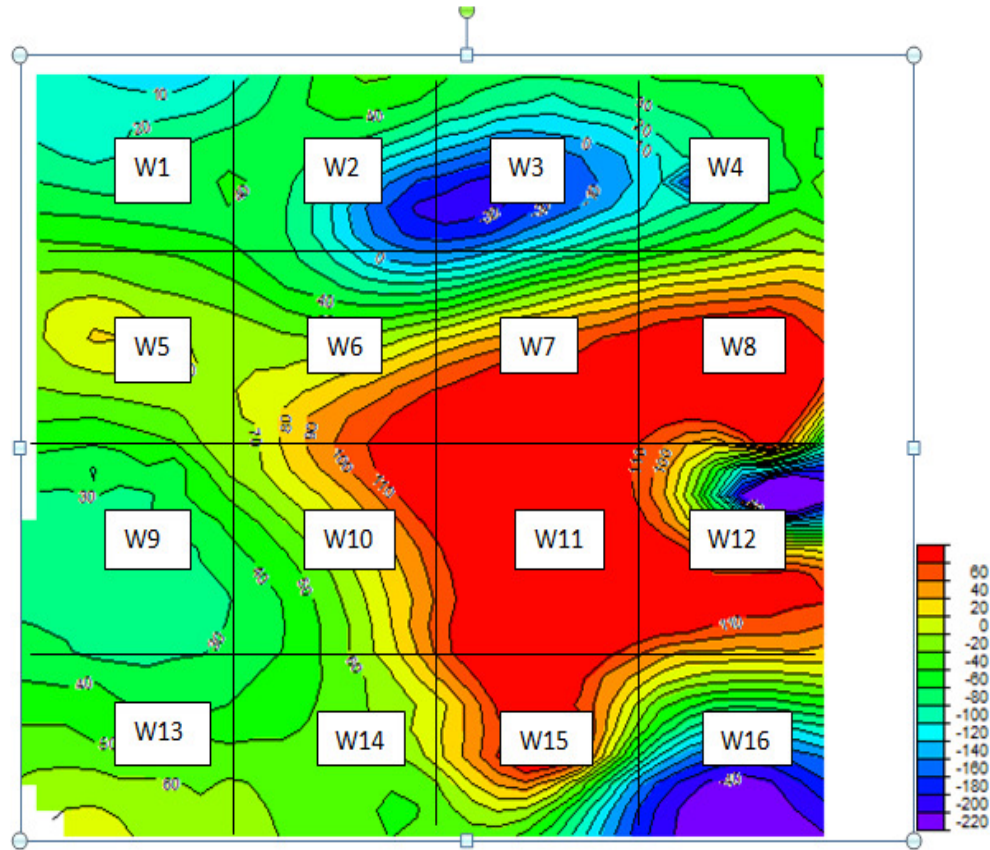
FAST FOURIER TRANSFORM (FFT) PERFORMED ON EACH SPECTRAL WINDOW

FFT mathematical modeling was performed on the 16 spectral aeromagnetic grids (or windows) of 10 km by 10 km for spectral depth analysis using the FFT function in the data analysis tool. For the FFT to be implemented, the 16 grids were imported into the Microcal OriginPro8 software for scientific data analysis and processing. The FFT function was used to separate the TMI data of the windows (called cells) into their frequency component and energy (FFT magnitude or the absolute value of the FFT complex) spectrum. Although, the data was smoothed using smoothing function of the Origin Pro 8. This was necessary since the computed logarithmic energy generally reveals a slowly decreasing mean value within an envelope of erratic rapid variations. The FFT was then performed on the Smoothed TMI data for all the cells. Hence, the discrimination of the anomalies into its energy spectrum and frequency component. To determine the spatial frequency component a sampling interval 1000 m was used applying square window with a one-sided spectrum type normalized to Mean Square Amplitude (MSA). This setting output the Spatial Frequency domain (cycle/m), FFT Complex, and energy (magnitude) spectrum. The log of the energy (Log E) was then plotted against the radial frequency in MS Excel as suggested by Spector and Grant (1970). A straight line is finally visually fit to the energy spectrum, usually in the higher and lower frequency of the figure. The negative of slope of this line is equal to twice the depth (depth = slope/2) to the center of mass of the bodies producing the magnetic field. After the depth has been calculated over one window a new calculation is made over a new window. This continues over the grid until all windows have had their radial spectra calculated and the depths picked.

ESTIMATION OF THE CURIE POINT DEPTH (CPD)

The method of Curie Point Depth determination utilizes spectrum analysis technique to separate influences of the different body parameters in the observed magnetic anomaly field¹¹. Two basic methods for estimating the CPD have been stated. They include those that examine the shape of isolated magnetic anomalies⁷ and those that examine the statistical properties and patterns of the anomalies²². These two methods, however, provide the relationship between the spectrum of the magnetic anomalies and the depth of a magnetic source by transforming the spatial data into frequency domain. This research adopted the method in which the top boundary and the centroid of magnetic sources were calculated from the spectrum of magnetic anomalies which were used to estimate the basal depth of magnetic

257 source. For the possible determination of the CPD, the residual data was divided into sixteen
258 (16) overlapping windows as shown below:



259

260 **Fig. 4: Sixteen (16) overlapping windows for CPD determination via spectral analysis**

261

262 Spectral analysis was thereafter performed on the sixteen windows. From the spectral depth
263 analysis the following steps were then undertaken

264 ➤ **STEP ONE:** Estimation of the depth to Centroid (Z_C) of the magnetic sources from
265 the slope of the low frequency component part of the energy spectrum.

266 ➤ **STEP TWO:** Estimation of the depth to the top boundary (Z_t) of magnetic sources
267 from the slope of the high frequency component part of the spectral segment.

268

269 The calculation of Z_C and Z_T then lead to the calculation of the basal depth Z_b using equation
270 1 and this is assumed^{23,24} as the CPD

271

272
$$Z_b = 2Z_C - Z_t$$

1

273

274 **Where**

275 Z_b = the basal depth

276 Z_c = the centroid depth

277

278 **HEAT FLOW AND THERMAL GRADIENT DETERMINATION**

279

280 A relation showing one dimensional heat conductive model was used for this study in order
281 to estimate the heat flow and the geothermal gradient in the absence of a heat flow data. This
282 model is based on the Fourier's law²³. Fourier's law is mathematically expressed as²³

283

$$284 \quad q = \lambda \frac{dT}{dz} \quad 2$$

285

286

287 Where

288

289 q = the heat flow

290 λ = the coefficient of thermal conductivity

291 $\frac{dT}{dz}$ = an assumed constant as no heat gain or loss above the crust and below the CPD

292 The Curie temperature (θ_c) is defined¹⁰ as

293

$$294 \quad \theta = \left[\frac{dT}{dz} \right] Z_b \quad 3$$

295

296 Equating 2 and 3, we have

297

298

299

$$300 \quad q = \lambda \left[\frac{\theta}{Z_b} \right] \quad 4$$

301

302 Equation 4 was therefore used in this research work in determining the heat when the Curie
303 point depths were known. For these estimations to be possible, a standard for curie point
304 isotherm of 580°C and thermal conductivity of 2.5 Wm⁻¹°C⁻¹ was used¹⁴. Finally, the
305 geothermal gradient was determined using equation 3, hence we have:

306

$$307 \quad \frac{dT}{dz} = \frac{\theta}{Z_b} \quad 5$$

308 Where

309 $\frac{dT}{dz}$ = geothermal gradient

310 Z_b = the basal depth

311 θ = the standard curie point isotherm of 580°C

312 Also, $\frac{dT}{dz}$ can be estimated by applying Fourier's model stated in equation 2, from equation 2
313 we have:

314

$$315 \quad \frac{dT}{dz} = \frac{q}{\lambda} \quad 6$$

316 Where

317 q = the heat flow

318 λ = thermal conductivity and is given as 2.5 Wm⁻¹°C⁻¹ for igneous rocks

319

320 RESULTS AND INTERPRETATION

321 In this work, quantitative analysis was achieved by using spectral depth analysis in
322 computing the depth to magnetic basement on each of the spectral windows. Performed on
323 each of the windows is FFT. The FFT modeling aided in decomposing each of the window
324 data set into its frequency components. Thereafter, plots showing log of energy (LogE)
325 versus the radial frequency were made. Based on the plots, table 1 which shows the centriod
326 depth (Z_C) and the depth to the top boundary (Z_t) of the magnetic sources was generated. The
327 Z_C is due to magnetic sources within the basement while the Z_T is due to magnetic sources
328 within the sedimentary section. In otherwords, Z_C and Z_t reflect magnetic sources due to deep
329 and shallow seated features. Z_C is a true reflection of Precambrian magnetic basement bodies
330 and these values ranges from -7.7 km to -12.0 km while Z_t possibly depicts magnetic effect
331 due to short wavelength sources and these ranges from - 0.5 km m to - 3.1 km.

332 Nevertheless, the CPD were computed and this work found out that this varies between -14.9
333 km and -23 km while the geothermal gradient and the heat flow varies from -25.2 to -37.9
334 °Ckm⁻² and -63 to -97.3 mWm⁻² respectively. Summary of the various windows with their
335 various parameters calculated are shown in Fig. 5.

336

337

338

339 **Table 1: Estimation of geothermal gradient and heat flow from CPD via spectral**
 340 **analysis**

WINDO W	SLOPE		DEPTH(km)			AVERA GE	GEO THERM AL	HEAT
						DEPTH (km)	GRADIENT	FLO W
	M ₁	M ₂	Z _c	Z _t	Z _b		(°Ckm ⁻²)	(mW m ⁻²)
W1	- 23995 .5	- 2011.4 7	-12	-1	-23	-6.5	-25.2	-63
W2	- 17762	- 1361.9 1	-8.9	-0.7	-17.1	-4.8	-33.9	-84.8
W3	- 23612 .7	- 3218.7 4	-11.8	-1.6	-22	-6.7	-26.4	-65.9
W4	- 18315 .6	- 2817.4	-9.2	-1.4	-17	-5.3	-34.1	-85.3
W5	- 19116 .1	- 2461.3 8	-9.6	-1.2	-18	-5.4	-32.2	-80.6
W6	- 20307 .3	- 3801.7 6	-10.2	-1.9	-18.5	-6	-31.4	-78.4
W7	- 21503 .2	- 2011.8 1	-10.8	-1	-20.6	-5.9	-28.2	-70.4
W8	- 19213 .4	- 3322.6 1	-9.6	-1.6	-17.6	-5.6	-33	-82.4
W9	- 22431 .8	- 1704.3	-11.2	-0.9	-21.5	-6	-27	-64.4
W10	- 18334 .1	- 6231.6	-9.2	-3.1	-15.3	-6.1	-38	-94.8
W11	- 15419 .3	- 1002.1 8	-7.7	-0.5	-14.9	-4.1	-38.9	-97.3
W12	- 17332 .5	- 2234.3 3	-8.7	-1.1	-16.3	-4.9	-35.6	-89
W13	- 21334 .1	- 5604.3	10.7	-2.8	-18.6	-6.8	-31.2	-78

W14	- 22332 .1	- 2101.3 8	-11.2	-1.1	-21.3	-6.2	-27.2	-68.1
W15	- 20119 .2	- 5770.2 8	10.1	-2.9	-17.3	-6.5	-33.5	-83.8
W16	- 15773 .2	- 997.08	-7.9	-0.5	-15.3	-4.2	-37.9	-94.8

341

342

WINDOW 1 $Z_b = -23$ $Z_c = -12$ $Z_t = -1$	WINDOW 2 $Z_b = -17.1$ $Z_c = -8.9$ $Z_t = -0.7$	WINDOW 3 $Z_b = -22$ $Z_c = -11.8$ $Z_t = -1.6$	WINDOW 4 $Z_b = -17$ $Z_c = -9.2$ $Z_t = -1.4$
WINDOW 5 $Z_b = -18$ $Z_c = -9.6$ $Z_t = -1.2$	WINDOW 6 $Z_b = -18.5$ $Z_c = -10.2$ $Z_t = -1.9$	WINDOW 7 $Z_b = -20.6$ $Z_c = -10.8$ $Z_t = -1.0$	WINDOW 8 $Z_b = -17.6$ $Z_c = -9.6$ $Z_t = -1.6$
WINDOW 9 $Z_b = -21.5$ $Z_c = -11.2$ $Z_t = -0.9$	WINDOW 10 $Z_b = -15.3$ $Z_c = -9.2$ $Z_t = -3.1$	WINDOW 11 $Z_b = -14.9$ $Z_c = -7.7$ $Z_t = -0.5$	WINDOW 12 $Z_b = -16.3$ $Z_c = -8.7$ $Z_t = -1.1$
WINDOW 13 $Z_b = -18.6$ $Z_c = -10.7$ $Z_t = -2.8$	WINDOW 14 $Z_b = -21.3$ $Z_c = -11.2$ $Z_t = -1.1$	WINDOW 15 $Z_b = -17.3$ $Z_c = -10.1$ $Z_t = -2.9$	WINDOW 16 $Z_b = -15.3$ $Z_c = -7.9$ $Z_t = -0.5$

343

344 **Fig. 5: Succinct view of the various windows and their various depths (km)**

345

346

347

DISCUSSION OF FINDINGS

Graphs of the spectral energies revealed that the depth due to the deep seated anomalous sources or the centroid depth (Z_c) varies from 7.7 km to 12.0 km. Conversely, the depth due to the shallow bodies or due to the top boundary of magnetic sources ranges between 0.5 km to 3.1 km while the corresponding CPD ranges from 14.9 km to 23.0 km. The true or average depths for each of the respective windows were calculated and this varies between 4.1 km and 6.1 km. Generally, a true depth of 5.3 km was ascertained within the study area. The depth value of 5.3 km suggests relative sedimentary thickness. These results compares favourably with the result of other researchers¹ within the lower Benue trough. Although with information on the crustal temperature missing in his work, He obtained the depths due to the deep seated sources to range from 7.2 km to 13.0 km while the depths values for the shallow sources varies from 0.4 km to 3.9 km, but on the average, he obtained a true depth of 7 km. Within parts of lower Benue trough, a thickness value of 5.6 km is believed to exist²⁵. This result is not a far cry from what was obtained for this study. Also, the CPD values¹³ were obtained within the area. The CPD depths were not in variance with those CPD values obtained for this study. However within the study area, the CPD within the study area vary from 23.80 km to 28.70 km. Shallower CPD can be seen towards the southeastern portion of the study area and this falls within the Oji river settlement province perceived to be the crystalline basement area. This is a possible reflection of the thinning of the crust under Benue rift¹³. They further stated that the basement area is as a result of the upwelling of magma on Cameroon Volcanic Line (CVL) during the tertiary period. Hence, the possibility of igneous intrusive that provide appropriate geothermal energy needed for the maturation of hydrocarbon found within that region. This particular findings is therefore in support of the fact that geo thermally active regions are usually shallower as it consist of igneous intrusive that could foster or be detrimental to hydrocarbon maturation. The heat flow within the study area varies between -64.4 mWm^{-2} and -97.3 mWm^{-2} but with an average of about 80.1 mWm^{-2} while the geothermal gradient varies from $25.2 \text{ }^{\circ}\text{Ckm}^{-2}$ to $38.9 \text{ }^{\circ}\text{Ckm}^{-2}$ but with an average of about $32.1 \text{ }^{\circ}\text{Ckm}^{-2}$ existing within the area under review. The heat flow values and the geothermal gradient values obtained further validate the fact that the shallowest depth occurring within window eleven (11) is a good geo thermally active area. Also, windows 2, 4, 8, 10, 12, 15 and 16 are possible geothermal resource areas. These areas will not, thus, be much productive in terms of oil and gas.

CONCLUSION

The study area is characterized with high heat flow and geothermal gradient with relatively low magnetic intrusions which could be detrimental to the quantity of hydrocarbon exploration. Therefore, the high heat flow and moderate geothermal gradient observed in this study is tectonically induced rifting and magmatism that occurred during Pan–African Orogeny.

REFERENCES

1. Umeanoh, D.C. 2015 Structural interpretation of aeromagnetic data over parts of lower benue trough, Nigeria, Msc thesis, University of PortHarcourt, Choba, Nigeria, (Unpubl).
2. Nettleton, L. L. 1971. Elementary Gravity and Magnetism for geologists and seismologists. Society of Exploration Geophysicists, Monograph series, (1) 121.
3. Reynolds, L. R., Rosenbaum, J. G., Hudson, M.R., and Fishman, N.S. 1990. Rock Magnetism, the distribution of magnetic minerals in the earth crust and aeromagnetic anomalies: U.S. Geological Survey and aeromagnetic anomalies: U.S. Geological Survey, Bulletin 1924, 24-45.
4. Tselentis, G.A. 1991. An attempt to define Curie depth in Greece from Aeromagnetic and heat flow data. PAGEOPH, 36(1), 87-101.
5. Ibrahim, A., Halil, I. and Ali, K. 2015. Curie-point depth map of Turkey. *Geophys. J. Int.*, 162(12), 633–640.
6. Vacquier, V. and Affleck, J. 1941. A computation of the average depth to the bottom of the Earth' magnetic crust, based on a statistical study of local magnetic anomalies. *Trans. Am. geophys. Un.*, 2, 446 – 450.
7. Bhattacharyya, B.K. and Leu, L.K. 1975. Analysis of magnetic anomalies over Yellowstone National Park: mapping of Curie point isothermal surface for geothermal reconnaissance, *J. geophys. Res.*, 80, 4461 - 4465.
8. Shuey, R.T., Schellinger, D.K., Tripp, A.C. and Alley, L.B. 1977. Curie depth determination from aeromagnetic spectra. *Geophys. J. R. astr. Soc.*, **50**, 75–101.
9. Connard, G., Couch, R. and Gemperle, M. 1983. Analysis of aeromagnetic measurements from the Cascade Range in central Oregon. *Geophysics*, **48**, 376–390.
10. Tanaka, A., Okuba, Y. and Matsubayashi, O. 1999. Curie point depth based on spectrum analysis of the magnetic anomaly data in East and Southeast Asia. *Tectonophysics*, **306**, 461–470.

- 422
- 423 11 Elleta, B.E. and Udensi, E.E. 2012. Investigation of the Curie point Isotherm from
424 the Magnetic Fields of Eastern Sector of Central Nigeria. *Geosciences*, 2(4): 101-106.
425
- 426 12 Hisarlı, M. 1995. Determination of the Curie point depths in Edremit - Susurluk
427 region (Turkey). *Jeofizik*, **1**(2), 111–117.
428
- 429 13 Nuri, D. M., Timur U. Z., Mumtaz, H. and Naci, O. 2005. Curie Point Depth
430 variations to infer thermal structure of the crust at the African-Eurasian convergence
431 zone, SW Turkey. *Journ.Earth planets Space*. 57(20), 373-383.
432
- 433 14. Nwankwo, L.I., Olasehinde , P.I. and Akoshile, C.O. 2011. Heat flow anomalies from
434 the spectral analysis of Airborne Magnetic data of Nupe Basin, Nigeria. *Asian Journal*
435 *of Earth Sciences*. 1. (1), 1-6.
436
- 437 15. Nur, A., Ofoegbu C.O. and Onuoha K.M. 1999. Estimation of the depth to the Curie
438 point Isotherm in the upper Benue trough, Nigeria. *Jour. Min. Geol.*, 35 (1), 53 - 60.
439
- 440 16. Onyewuchi, A.R. 2011 Interpretation of Aeromagnetic and Landsat Imageries of
441 Okposi, Ebonyi State, SE Nigeria, Msc thesis, University of PortHarcourt, Choba,
442 Rivers State, (Unpubl).
- 443 17. Murat, R.C. 1972. Stratigraphy and paleogeography of the Cretaceous and lower
444 Tertiary in southern Nigeria. *African Geology*, University of Ibadan Press, 251-266.
- 445 18. Nwozor, K.K., Chiaghanam, O.I., Egbuachor, C.J. and Onyekuru, S.O. (2012):
446 Surface Geophysics Character of Maastrichtian - Danian Sediments in parts of Udi-
447 Ezeagu Area, Southern Anambra Basin, Nigeria. *Archives of Applied Science*
448 *Research*, 4 (4):1609-1617.
- 449 19. Hahn, A.; Kind, E.G. and Mishra, D.C. 1976. Depth estimation of Magnetic Sources
450 by means of Fouries amplitude spectra. *Geophysical Prosp.* 24: 278-308.
451
- 452 20. Odegard, M.E. and Berg, J.W. 1975. Gravity interpretation using Fourier integral.
453 *Geophysics*, 32(4), 1-4.
- 454 21 Blakely,R.J. 1996. Potential theory in gravity and Magnetic Applications. Cambridge
455 University Press, New York, 435-567.
- 456 22 Spector, A. and Grant, F.S. 1970. Statistical models for interpreting aeromagnetic
457 data, *Geophysics*, 35, 293- 302.
458
- 459 23 Kasidi, S. and Nur, A. 2012. Curie depth isotherm deduced from spectral analysis of
460 Magnetic data over sarti and environs of North-Eastern Nigeria. *Scholarly J.*
461 *Biotechnol.* 1(3), 49-56.
462
- 463 24 Okubo,Y.J., Graf, R., Hansen, R.O., Ogawa, K. and Tsu, H. 1985. Curie point depth
464 of the Island of Kyushu and surrounding areas. *Japan Geophysic.*, 53, 481-491.

465

466 25 Onwumemesi, A.G. 1996. One-dimensional spectral analysis of aeromagnetic anomalies
467 and curie depth isotherm in the Anambra basin of Nigeria. J. Geodynamics, 23(2), 95-
468 107.